UNIVERSIDADE DE SÃO PAULO

INSTITUTO DE FÍSICA
CAIXA POSTAL 66318
05315-970 SÃO PAULO - SP
BRASIL

PUBLICAÇÕES

IFUSP/P-1303

Nymo: 2179545

NONLINEAR MODELS FOR DETECTING EPILEPTIC SPIKES

L. Diambra and **C.P. Malta**
Instituto de Física, Universidade de São Paulo

Março/1998

Nonlinear Models for Detecting Epileptic Spikes

L. Diambra*, and C.P. Malta

Instituto de Física, Universidade de São Paulo,

C.P. 66318, cep 05315-970, São Paulo, SP, Brazil

Abstract

We present a technique for automatic detection of epileptic spikes in electroencephalogram (EEG) recordings. We use a nonlinear modeling method based on Information Theory (IT) that enables us to detect rapidly and accurately epileptic behaviour in the EEG signal. An optimal embedding dimension of the model is determined by the minimum in the mean square relative error between EEG signals and the corresponding model prediction. Our approach is illustrated by an application to two EEG time series: (i) interictal activitity from focal epileptic patient, and (ii) a *petit male* from generalized epilepsy patient.

PACS number: 87.10.+e, 05.45.+b

Typeset using REVTEX

*Electronic address: diambra@linpel.if.usp.br

I. INTRODUCTION

During recent years several neurophysiological studies have shown that electroencephalogram (EEG) signals have high degree of complexity resulting from either random processes or chaotic behavior generated by nonlinear dynamical systems [1,2].

One of the most important uses of the traditional visual interpretation of the EEG is the identification of transient events associated with epilepsy, where the background activity is interrupted by sharp waves or spikes [3,4]. Sharp waves and spikes recorded in the periods between seizures (interictal activity) are of great importance for diagnosis purpose. The morphology and topography of these sharp transients have been correlated with different types of seizure [5]. Epileptic seizures can be focal or generalized. In focal epilepsy the seizure begins in a restricted brain region and either remains localized or spreads to adjacent cortex, while in generalized epilepsy the seizure involves all the brain. The interictal activity (IA) of focal epilepsy is also localized, while in generalized epilepsy this activity is recorded in the whole cortex [3].

The community of neurophysiological researchers has concluded that EEG signals stem from a highly nonlinear system [1,2,6]. In this context, several methods based in linear (spectral analysis) and nonlinear measures have been applied to quantitative EEG analysis [6–12]. Distances between points in appropiate embedding space of the data are used to compute a set of metric parameters of nonlinear dynamics analysis, such as: correlation dimension, Lyapunov exponents, Kolmogorov entropy [13–15]. For a reliable estimation of these parameters, large quantities of data (about 10^d where d is the embedding dimension [16]) are necessary to achieve accurate approximations for the density of points in different regions of the attractor. Thus, long (between 1000 to 10000 points) stationary time series [17] of EEG signals are required by those methods. In most of the cases, the stationarity of the signal is usually taken for granted, although this condition may not be satisfied when we deal with EEG signals [9], since stationary intervals are of the order of ten seconds (1000 points of standard clinical EEG), depending on the behavioral state [18]. Moreover, these

methodologies are not useful for an accurate temporal localization of transient events in EEG recording. In contrast, the approach presented here is able to characterize the dynamics of short portions of signals.

In this communication, we assume that different behavioral states are characterized by different dynamics in the EEG. In Fact, EEG signals from vigilia state can be described as linearly filtered noise [7]; while many authors have reported evidence that epileptiform EEG signals may exhibit low dimensional deterministic chaos [12,19,20]. We assume that epileptic EEG signals are basically deterministic chaos with some level of additive random noise. This means that the dynamical evolution of the system could be described, basically, by few variables and one can construct a model able to predict the short future behavior of the system in terms of its previous states [21,22].

In the present effort, we examine the possibility of applying a nonlinear prediction approach for automatically detecting the interictal activity (IA) spikes in EEG. We compare the ability of prediction of a model constructed from segments without IA, when applied to an interval containing IA spikes. As the dynamics with IA differs from the dynamics without IA, we expect a poor prediction power. In this way, we can use some estimator of the performance, in order to detect IA spikes. The models one is interested in must be able to predict on the basis of adequately selected *working hypothesis*. This hypothesis is represented by a set of parameters of the model. We apply Information Theory (IT) techniques, within the framework of Maximum Entropy Principle (MEP) [23–25], in order to select the working hypothesis of the model. Some preliminary considerations in this direction have been advanced in [26].

The automatic detection of epileptic spikes can be particularly valuable in dealing with focal epilepsy, specially when surgical treatment is indicated [27]. The methodology presented here has advantages over the calculation parameters based on distances because it presents an effective temporal localization, and it uses a short stationary interval (3 to 4 seconds of standard clinical EEG). The computational burden is significantly lower and can be implemented on-line with the acquisition of the signal. An effective temporal localization

is useful for the spatial estimation of epileptogenic focus [27,28].

We organize our presentation as follows: in Sec. II we review some ideas concerning both reconstruction of the system's state, and IT based parameters estimation procedure. We describe also the procedure used to record the EEG signals. In Sec. III we present our results regarding the EEGs of patients with IA and *petit male*. Finally some conclusions are drawn in Sec. IV.

II. METHOD AND DATA

A. Nonlinear prediction approach

We shall present briefly the IT-based method for building a deterministic model. We assume that the EEG signal is a stroboscopic sequence of N measurement $\{v(t_0), v(t_0+\tau_s), \ldots, v(t_0+N\tau_s)\}$ made at intervals τ_s, and reconstruct the state space using time delay embedding [29,30], which uses a collection of coordinates with time lag to create a vector in d dimensions,

$$\mathbf{v}(t_n) = (v(t_n), v(t_n-\Delta), \ldots, v(t_n-(d-1)\Delta)), \tag{1}$$

where $\Delta = n\tau_s$, $(n \in \mathcal{N})$, is the time lag or delay. Takens has shown [29] that, for flows evolving to compact attracting manifolds of dimension d_a, if $d > 2d_a$, we can write

$$v(t+T) = F(\mathbf{v}(t)), \tag{2}$$

where $T > 0$ is the forecasting time. This theorem provides no information regarding either the choice of Δ, or the form of F.

Now, we introduce the IT ideas for building a deterministic model depending on parameters. The implementation of this idea is to build parametrized functions $F^*(\mathbf{v}(t), \mathbf{a})$, where $\mathbf{a}$ is the set of parameters of the model. Then, we use MEP criteria, i.e., the minimum number of assumptions compatible with the available data, to determine the set of parameters

a that constitutes the working hypothesis. The motivation for this criteria is to reduce the length of time series necessary for building a model with good predictive ability.

We consider a representation of the mapping function $F^*(\mathbf{v})$ as an expansion in the form

$$F^*(\mathbf{v}) = \sum_{j=1}^{d} \sum_{i=1}^{p} a_{ij} \exp\left[-\frac{p}{2}(v_j - x_i)^2\right] \tag{3}$$

where v_j are the components of the d-vector (1), and x_i are the coordinates of p equidistant points (we take $x_i \in [-1.5, 1.5]$ in a signal normalized to unity). Of course, a_{ij} constitute our working hypothesis. Thus, the number of parameters of the model N_c, is determined by the number of Gaussian functions p in (3), and by the embedding dimension d, $N_c = d \times p$.

The idea is now to introduce the MEP [26] in order to determine the parameters $\mathbf{a} = \{a_{11}, a_{12}, \ldots, a_{pd}\}$ using the information contained in M points of EEG

$$\{\{v_1(t_n), v_2(t_n), \ldots, v_d(t_n)\}, v(t_n + T)\}, \tag{4}$$

where $n = 1, \ldots, M$.

In order to infer the coefficient consistent with the data set (4) we shall assume that *each set* **a** *is realized with probability* $P(\mathbf{a})$. Of course, $\int P(\mathbf{a}) d\mathbf{a} = 1$, where $d\mathbf{a} = da_{11} da_{12} .... da_{pd}$. Expectation values $\langle W_i \rangle$ are defined, as usual,

$$\langle a_i \rangle = \int P(\mathbf{a}) a_i d\mathbf{a}, \tag{5}$$

and a *relative* entropy is, in the usual way [23,24], associated to the probability distribution, namely,

$$S = -\int P(\mathbf{a}) \ln\left(\frac{P(\mathbf{a})}{P_0(\mathbf{a})}\right) d\mathbf{a}, \tag{6}$$

where $P_0(\mathbf{a})$ is an appropriately chosen *a priori* distribution [24,25]. Our *central* idea is that we reinterpret the data set (4), according to the expression (3)

$$v(t_n + T) = \langle \mathbf{a} \rangle \cdot \mathbf{V}, \tag{7}$$

where $\mathbf{V}$ is a vector constructed by evaluation of p Gaussian functions (3) in each component of the d-vector $\mathbf{v}$.

As customary [24], one is then led to maximizing the entropy (6) subject to constraints (7) and the normalization condition, obtaining

$$S' = -\int \left\{ P(\mathbf{a}) \ln\left(\frac{P(\mathbf{a})}{P_0(\mathbf{a})}\right) + \lambda_0 P(\mathbf{a}) + \mathbf{W}^t \overrightarrow{\lambda} \cdot \mathbf{a} P(\mathbf{a}) \right\} d\mathbf{a}, \tag{8}$$

where λ_0 and $\overrightarrow{\lambda}$ are Lagrange multipliers associated, respectively, to the normalization condition and the constraints (7), and $\mathbf{W}$ is a matrix with M rows $\mathbf{V}(n)$. Variation of S' with respect to $P(\mathbf{a})$ immediately gives

$$P(\mathbf{a}) = \exp(-(1 + \lambda_0)) \exp(-\mathbf{\Gamma} \cdot \mathbf{a}) P_0(\mathbf{a}), \tag{9}$$

where $\mathbf{\Gamma} = \mathbf{W}^t \overrightarrow{\lambda}$ ($\mathbf{W}^t$ is the transpose of $\mathbf{W}$).

A choice has now to be made concerning the *a priori* probability distribution P_0. Here we select a Gaussian P_0, i.e. choose it to be proportional to $\exp(-\mathbf{a}.\mathbf{a}/2\sigma)$, with a free parameter σ. When we replace this choice of the *a priori* distribution in eq. (9), we obtain a Gaussian form for the probability distribution $P(\mathbf{a})$, centered in $\langle \mathbf{a} \rangle = -2\sigma\mathbf{\Gamma}$, with dispersion σ. Both the definition of $\mathbf{\Gamma}$ and the constraints (7) allow for the elimination of the Lagrange multipliers $\overrightarrow{\lambda}$. One can thus express the $\langle a_i \rangle$, solely in terms of the data set:

$$\langle \mathbf{a} \rangle = v(t_n + T) I_{ps}[\mathbf{W}], \tag{10}$$

where $I_{ps}[\mathbf{W}] = (\mathbf{W})^t \left(\mathbf{W}(\mathbf{W})^t\right)^{-1}$ is Moore-Penrose pseudo-inverse [31]. Now, we choose the most probable set of parameters (the mean value of the distribution) compatible with the constraints (7) as our working hypothesis. In this way, one can capture the dynamics underlying a short portion of the EEG.

B. Clinical Data

The human individuals digital recordings have been obtained from: i) two adult patient with focal epilepsy at sleep stage 1-2. The epileptic focus was localized at the occipital EEG

derivations, ii) a 12 years old patient with *petit male* at sleep stage 1-2. The recordings have been obtained with a standard clinical device with 16 channels with a reference electrode placed at the patient's nose. Sample rate (τ_s^{-1}) has been of $102.5Hz$ and the low pass filter has been of $51.25Hz$. We used the recordings of the occipital channel in both EEG time series, so as to test our prediction technique.

III. RESULTS

Our procedure for the automatic detection of epileptic spikes will be illustrated with reference to two situations: during interictal activity from the two patients with focal epilepsy, and during a seizure from the patient with *petit male* epilepsy (as mentioned above, in both cases we use the occipital channel). One portion of the EEG signal (normalized to unit) is employed for adjusting the parameters of the model which is then used in a larger portion of the EEG signal for testing its predictive power. We expect good predictive performance when the dynamics of the EEG interval used for building the model is similar to the dynamics of the interval used for testing. A poor forecasting indicates that the system has changed its dynamics.

In order to build the model it is necessary to determine its embedding dimension d. To this end, we have analyzed the performance of the models for different embedding dimensions. The model incorporates five Gaussian functions, [see eq. (3)], and the time lag used is one sample ($\Delta = \tau_s$). We compute the mean relative error (MRE), between the EEG signal (v_j) and the forecasting (v_j^*) as a function of the embedding dimension. The MRE is defined by

$$MRE = N^{-1} \sum_j^N \frac{\left(v_j - v_j^*\right)^2}{v_j} \quad , \tag{11}$$

and we shall see that it exhibits a minimum when the embedding dimension reaches a certain value, this value depending on the signal nature. We choose the dimension corresponding to the minimum of the MRE as the embedding dimension of the model. We used two different

lengths of segment (300 and 400 points) for the modeling and EEG segments exhibiting different dynamics. In all cases the adequate embedding dimension was robust with respect to the number of points used in the modeling. In the Fig. 1, corresponding to a patient with focal epilepsy during IA, the MRE minimum is reached at $d = 4$ for all the 4 models considered (2 of the models used 400 points and the other 2 used 300 points). This result is in clear contrast with the case of EEG signal without epileptic activity. For comparison we show in the Fig. 2 the MRE *versus* embedding dimension computed on an EEG segment without IA (interval recorded 2 min. before the interval used in the Fig. 1) where clearly we cannot see any minimum at low dimensionality (here also 2 curves resulted from models with 400 points and the other 2 from models with 300 points). Thus a short portion of the EEG provides an effective characterization of its dynamics.

Fig. 3 corresponds to the case of the EEG signal from the patient with *petit male*, during the seizure. In this case the MRE minimum is at $d = 3$. In fact, as many authors have reported using other techniques, low dimensionality is due to a complexity decrease in the EEG during the seizure. The main advantage of our technique is that we use only 3 or 4 seconds of standard clinical recordings in order to characterize the loss of complexity. This is a remarkable facet of our approach because, when we deal with EEG signal, it is difficult to obtain a long transient for a reliable estimation of the parameters like correlation dimension or Lyapunov exponents.

We shall now present the result for the various models obtained using different segments of the EEG recording with the appropriate embedding dimension d as determined above for the regions with epileptic activity. In the regions of the EEG signal without epileptic activity we shall use $d = 11$ which corresponds to the value of d at which the MRE starts to saturate (see Fig. 2).

In Fig. 4 we display the results for one of the cases in which the EEG exhibits IA spikes (it is the case used in the Fig 1). The EEG recording is displayed at the top of the Fig. 4. The graph in the middle of Fig. 4 displays the prediction error from a model that was built using the first 400 points (region without IA spikes) of the EEG signal shown at the

top of figure 4. The embedding dimension used was $d = 11$ (see Fig. 2). We can clearly see huge sharp peaks, related to big errors (notice that the scale of this plot was zoomed up 10 times) at the points where IA spikes occur. In the graph at the bottom of the Fig. 4 we can see the concomitant prediction error from a model constructed using 400 points of the region with IA spikes (between 1350 and 1750). The model has dimension $d = 4$ (see Fig 1). In this case the amplitude of the peaks in the prediction error is considerably smaller than before. Moreover we do not see a signicant peak in the error in the region without IA (the model was made using an IA segment) where one would expect bigger errors.

We can conclude that these kind of models (deterministic models) can capture some aspects of the dynamics but not all of them, due to the presence of a stochastic component in the EEG signal. Nevertheless, as we can see from the Fig. 4, given a model constructed using a segment without IA spikes, if we compute its predictive performance in segments with IA spikes, these spikes can be detected clearly, by means of the peaks localization in the prediction error.

In Fig. 5, we can see the case of the other patient with focal epilepsy. We found the same results using different segments of the EEG as done in the case of the Fig. 4. In order to further test our method, we applied to the signal displayed at the top of Fig. 5, the two models used for constructing the Fig. 4. The corresponding prediction errors are displayed in the Fig. 6. As we can see, the result is essentially the same as shown in the Fig. 5. This means that the present method is robust in the sense that the model can be constructed once and for all using the signal of one patient, and provided the signals are normalized, the same model can be used for analysing other patients EEG signal.

The automatic detection of epileptic spikes is not specific of the focal epilepsy, the peaks in the prediciton error also occur in the spikes of generalized epilepsy. We applied this technique to *petit male* epilepsy, shown at the top of Fig. 7. In the middle of the Fig. 7 we show the prediction error from a model, with embedding dimension $d = 11$, which was constructed using the 400 points in a region without seizure (between 1300 and 1700). Again, we can see clearly sharp peaks, related to big errors in the seizure segment. At the

bottom of Fig. 7, we can see the concomitant errors from a model with $d = 3$ (see Fig. 3) constructed using 400 points in a region with seizure (between 600 and 1000). In this case, as in the case of the plot at the bottom of figures 4, 5 and 6, the error does not show sharp peaks.

IV. DISCUSSION AND CONCLUSIONS

We have presented here a new method, based on deterministic IT-modeling of EEG signals, for automatically detecting IA spikes. By suitably adjusting the dimension our model is able to "capture" the essential correlations of the system. The ratio between the amplitude of the peaks and the background error signal is greater than the ratio between the amplitude of the spikes and the background EEG. Our method can be implemented in the online-detection of IA when many hours of EEG recording are needed for a reliable diagnosis.

A remarkable fact is to be emphasized: the rather *small* quantity of points needed for the modeling. Thus the problems associated with the nonstationarity of the EEG signals are avoided. This means that the detection power, using the error signal, is good enough without loss of temporal resolution. In dealing with focal epilepsy, the high temporal resolution is particularly valuable because it improves the possibility of localizing and monitoring the epileptic focus activity using a multi-channel EEG recording [28].

We conclude by pointing out that the application of deterministic nonlinear models to the analysis of complex signals should receive renewed impetus from the present considerations. Moreover, these results corroborate the conjeture that epileptical activity could correspond to low dimension chaotic attractor, while the nature of normal EEG continues an open question.

V. ACKNOWLEDGMENTS

L. D. acknowledges the financial support of CNPq, Brazil, and C. P. M. acknowledges partial financial support by CNPq. The authors want to thank Daniel Lorenzo and Alberto Capurro both for providing the EEG signals and for the useful comments concerning their clinical interpretation.

REFERENCES

[1] S.A.R.B. Rombouts, R.W.M. Keunen, and C.J. Stam, Phys. Lett. A **202,** 352 (1995).

[2] W.S. Pritchard, D.K. Duke, and K.K. Krieble, Psycophysiology **32**, 486 (1995).

[3] A. Gevins, A. Rémond (Eds.), in *Handbook of Electroencefalography and Clinical Neurophysiology*, Vol I. (Elsevier, Amsterdam, 1987).

[4] E. Niedermeyer and F. Lopes da Silva (Eds.), in *Electroencefalography: Basic Principles, Clinical Applications and Related Fields*, (Urban and Schwarzenberg, Baltimore, 1983).

[5] E. Niedermeyer, in *Electroencefalography: Basic Principles, Clinical Applications and Related Fields.* Edited by E. Niedermeyer and F. Lopes da Silva (Urban and Schwarzenberg, Baltimore, 1983) p 115.

[6] J. Feller, J. Roeschke, K. Mann, and C. Schaeffner, Electroenceph. and Clin. Neurophysiol. **98**, 401 (1996).

[7] J. Theiler and P.E. Rapp, Electroenceph. and Clin. Neurophysiol. **98**, 213 (1996).

[8] C.J. Stam, T.C.A.M. vam Woerkon, and W.S Pritchard, Electroenceph. and Clin. Neurophysiol. **99**, 214 (1996).

[9] J.P.N. Pijn, J. Van Neerven, A. Noest, and F. Lopes da Silva, Electroenceph. and Clin. Neurophysiol. **79**, 371 (1991).

[10] A.P. Anokhin, N. Birbaumer, W. Lutzenberger, A. Nicolaev, and F. Vogel, Electroenceph. and Clin. Neurophysiol. **99**, 63 (1996).

[11] J.E. Arle and R.H. Simon, Electroenceph. and Clin. Neurophysiol. **75**, 296 (1990).

[12] A. Babloyantz and Destexhe, Proc. Natl. Acad. Sci. USA **83**, 3513 (1986).

[13] P. Grassberger and I. Procaccia, Phys. Rev. Lett. **50,** 346 (1983).

[14] J. Van Nerveen, Master's thesis. Dept. Exp. Zoology, Univ. of Amsterdam, Amsterdam,

1988.

[15] A. Wolf, J.B. Swift, H.L. Swinney, and J.A. Vastano, Physica D **16**, 285 (1985).

[16] J. Theiler, Phys. Rev. A. **41**, 3038 (1990).

[17] A.M. Albano, A.F. Mees, G.C. de Gusman, and P.E. Rapp, in Chaos in Biological Systems, edited by H. Degn, A. Holden, and L.F. Olsen (Plenum, New York, 1987), pp 207-219.

[18] F. Lopes da Silva, in *Electroencefalography: Basic Principles, Clinical Applications and Related Fields*, Edited by E. Niedermeyer and F. Lopes da Silva (Urban and Schwarzenberg, Baltimore, 1987) p 871-897.

[19] P.E. Rapp, L.D. Zimmerman, A.M. Albano, G.C. de Gusman, and N.N. Greenbaum, Phys. Lett. A **110**, 335 (1985).

[20] I. Dvorak and J. Siska, Phys. Lett. A **118**, 63 (1986).

[21] M. Casdagli, Physica D **35**, 335 (1989).

[22] M. Giona, F. Lentini, and V. Cimagalli, Phys. Rev. A **44**, 3496 (1991).

[23] C.E. Shannon and W. Weaver, in *The Mathematical Theory of Communication* (University of Illinois Press, Chicago, 1949).

[24] E.T. Jaynes, Phys. Rev. **106**, 620 (1957); Phys. Rev. **108**, 171 (1957).

[25] R.D. Levine and M. Tribus, in *The Maximum Entropy Principle* (MIT Press, Boston MA 1978).

[26] L. Diambra and A. Plastino, Phys. Lett. A **216**, 278 (1996).

[27] J. Gotman, R.G. Burges, T.M. Darcey, R.N. Herner, J.R. Ives, R.P. Lesser, J.P.M. Pijn, and D. Velis. In *Computer Applications, Surgical Treatment of Epilepsies,* edited by J. Engel Jr. (Raven Press Ltd. New York, 1993)

[28] D.E. Lerner, Physica D **97**, 563 (1996).

[29] F. Takens, in *Dynamical systems and Turbulence*, edited by D. Rand and L.S. Young, Lecture notes in Mathematics, Vol 898 (Springer, Berlin, 1981) p.366.

[30] H.D.I Abarbanel, R. Brown, J.J. Sidorowich, and L.S.Tsimring, Rev. Mod. Phys. **65**, 1331 (1993).

[31] A. Albert. In Regression and Moore-Penrose Pseudoinverse, (Academic Press, New York, 1972).

FIGURE CAPTIONS

Figure 1 MRE as a function of the embedding dimension for the EEG signal shown at the top of the Fig. 4. All the curves refer to models using segments with IA. Two of the curves correspond to models constructed using 400 points and the other two to models constructed using 300 points. The models were tested over the following 1000 points which also lie in a region with IA. Delay is one sample ($\Delta = \tau_s$), and we used $p = 5$.

Figure 2 MRE as a function of the embedding dimension for the EEG without epileptic activity. Two of the models were constructed using a segments of 400 points and the other two using segments of 300 points, and then they were tested over 1000 points of a subsequent interval (without IA). Delay is one sample, and we used $p = 5$.

Figure 3 MRE as a function of the embedding dimension for the EEG with *petit male* shown at the top of Fig. 7. all the curves refer to models using seizure segments. Two of the models were constructed using 400 points and the other two using 300 points, and then they were tested over the whole segment with seizure (1-1000). Delay is one sample, and we used $p = 5$.

figure 4 Top: 3 seconds of the EEG recording from a patient with focal epilepsy. Middle: prediction error from the model constructed using the first 400 points (without

IA spikes) with embedding dimension $d = 11$. Bottom: prediction error from the model using the 400 points with IA spikes (between 1350 and 1750) with embedding dimension $d = 4$.

figure 5 Top: 3 seconds of the EEG recording from another patient with focal epilepsy. Middle: prediction error from the model constructed using the first 400 points (without IA spikes) with embedding dimension $d = 11$. Bottom: prediction error from the model constructed using 400 points with IA spikes (between 1800 and 2200) with $d = 4$.

figure 6 Prediction errors for the EEG displayed at the top of the Fig. 5, using the same models of the Fig 4. Top: prediction error from the model without IA of Fig. 4 (to be compared with the prediction error displayed in the middle of the Fig. 5). Bottom: prediction error from the model with IA of Fig. 4 (to be compared with the prediction error displayed at the bottom of the Fig. 5).

figure 7 Top: 3 seconds of the EEG recording from a patient with *petit male*. Middle: prediction error from the model constructed using 400 points without epilepsy activity (between 1300 and 1700) with $d = 11$. Bottom: prediction error from the model constructed using 400 points with IA spikes (between 600 and 1000) with $d = 3$.

FIGURES

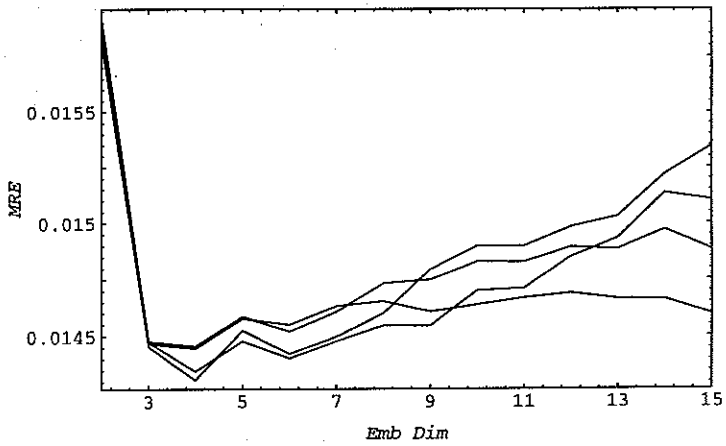

FIG. 1. L. Diambra and C.P. Malta

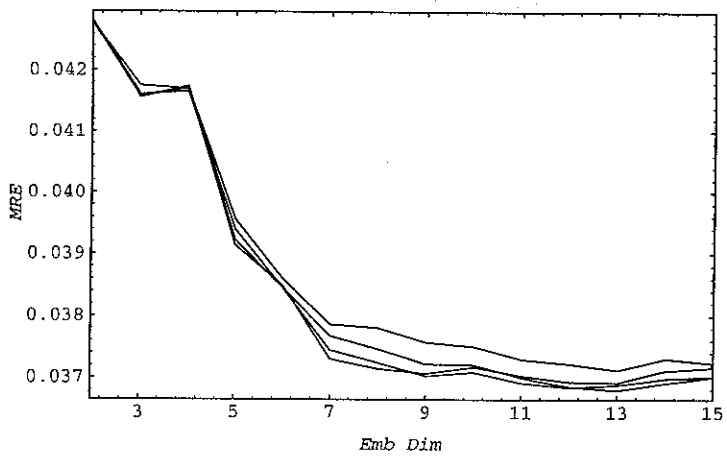

FIG. 2. L. Diambra and C.P. Malta

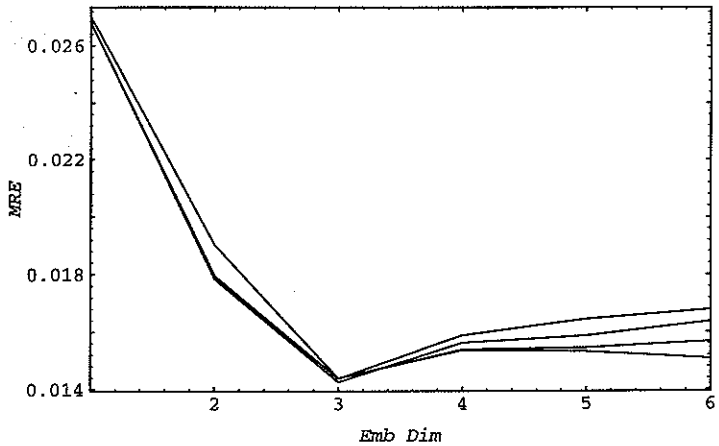

FIG. 3. L. Diambra and C.P. Malta

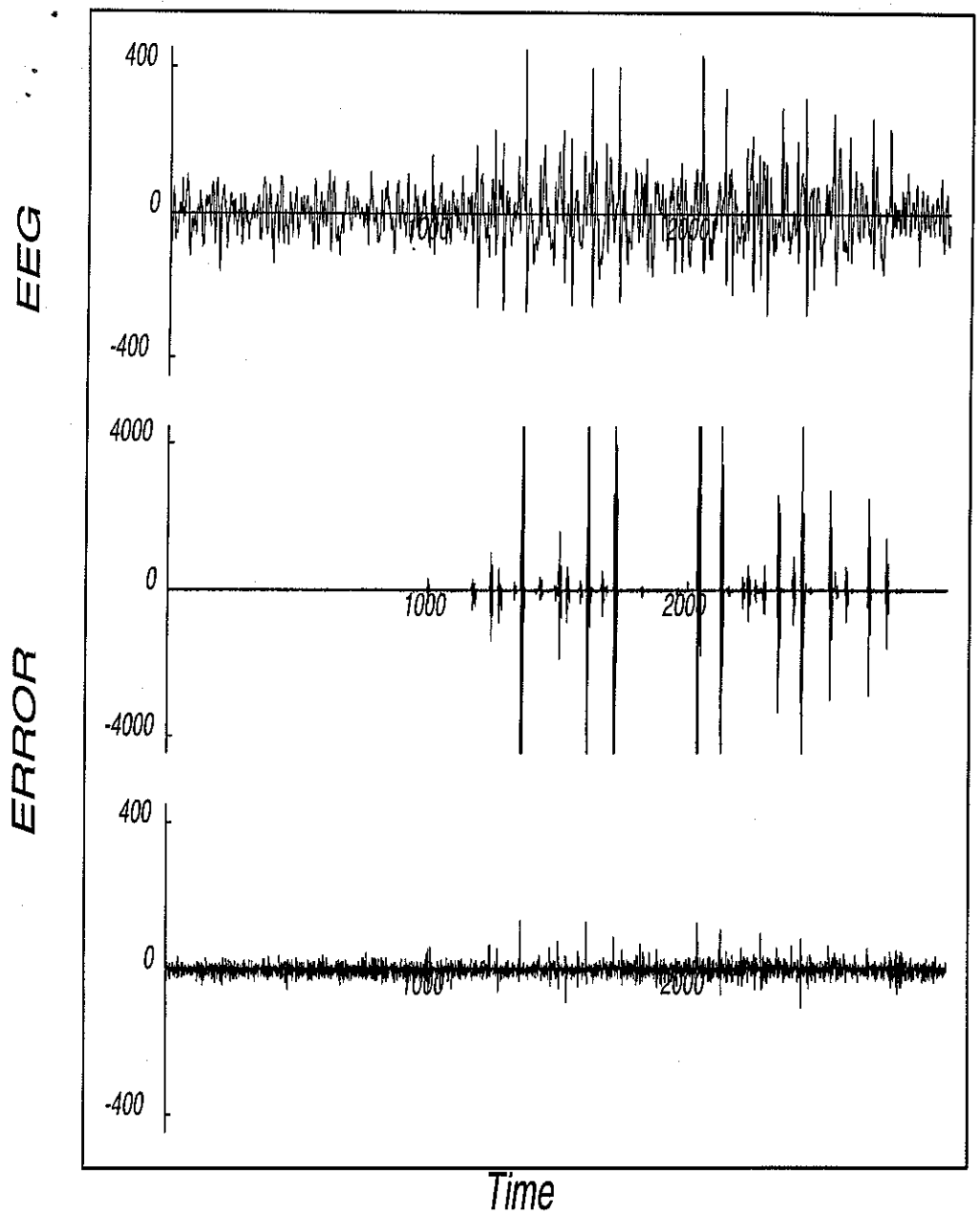

FIG. 4. L. Diambra and C.P. Malta

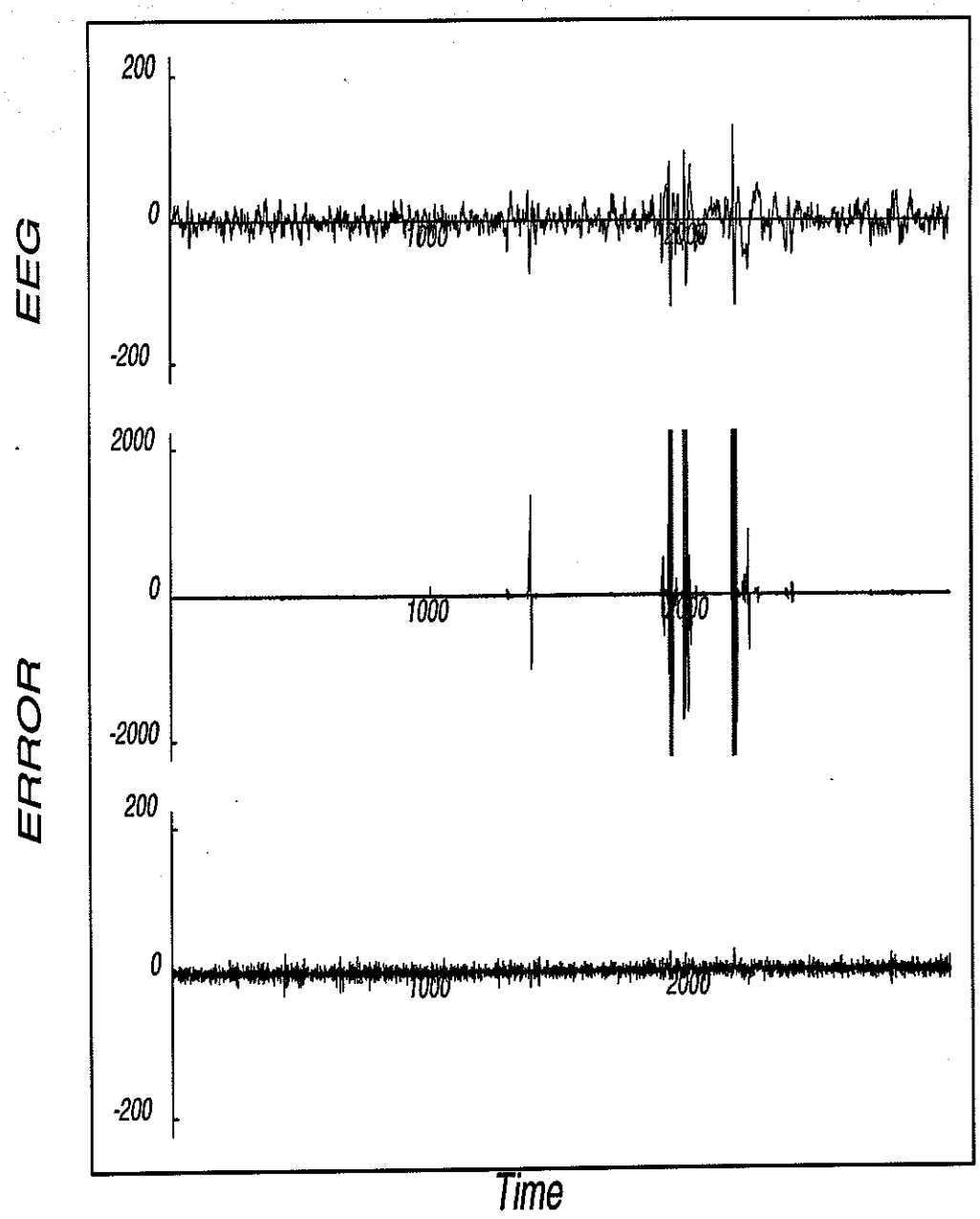

FIG. 5. L. Diambra and C.P. Malta

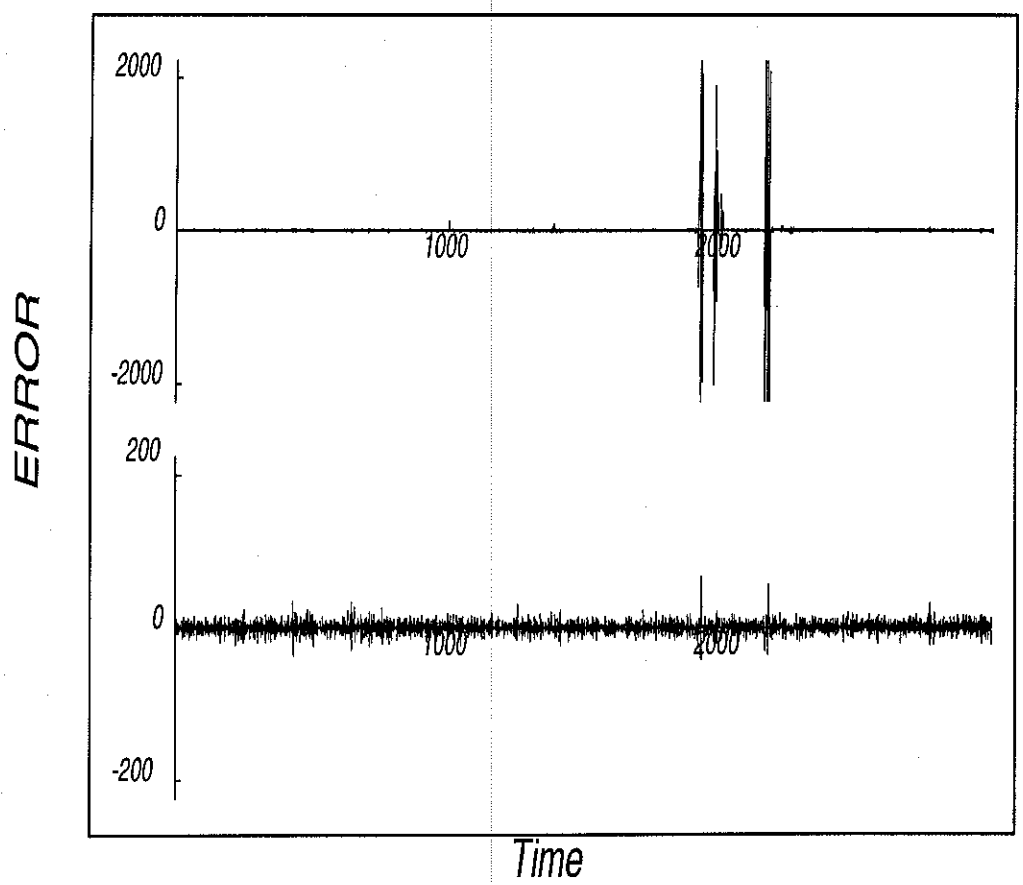

FIG. 6. L. Diambra and C.P. Malta

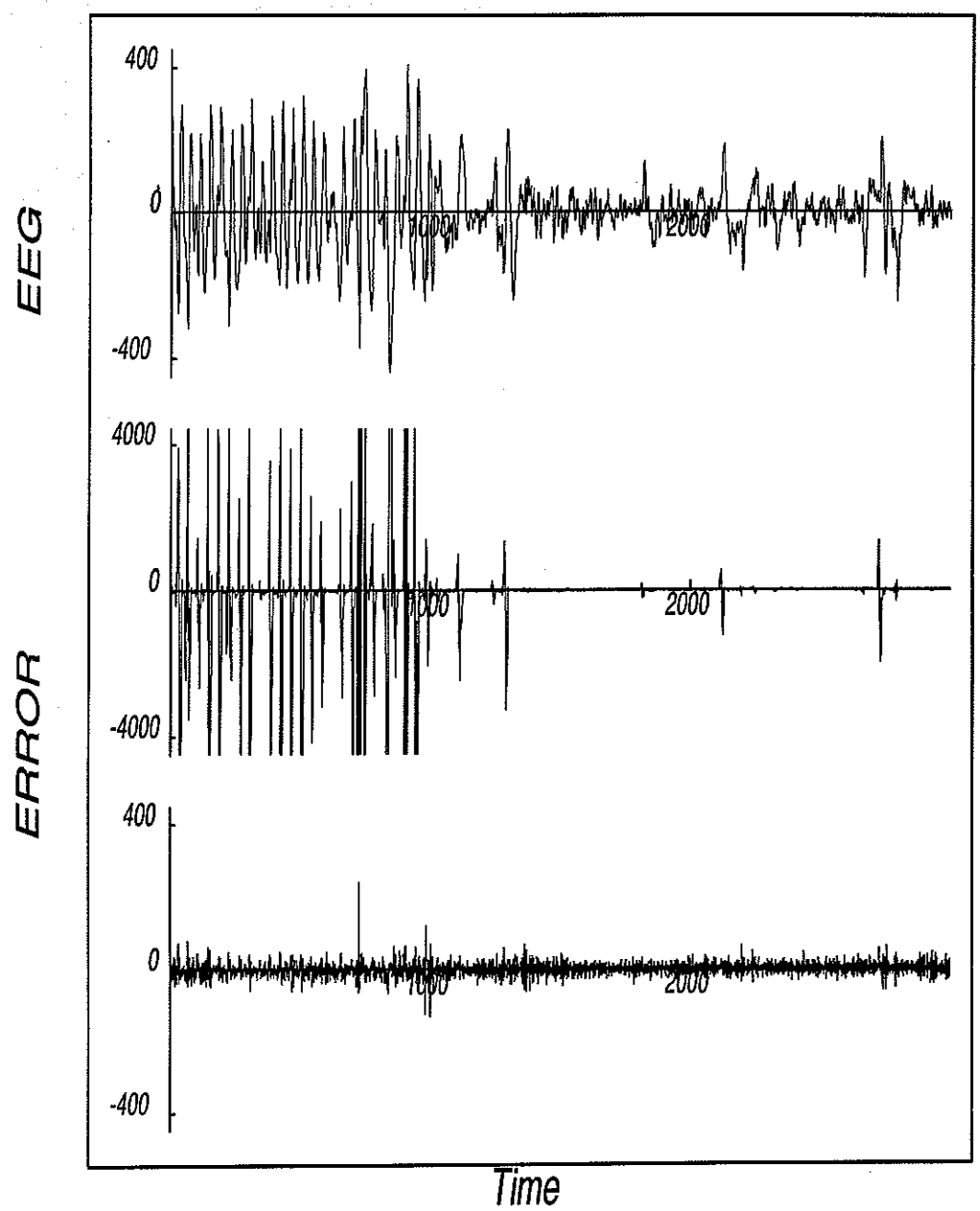

FIG. 7. L. Diambra and C.P. Malta